Assessing wave-turbulence separation from ADCP measurements with artifical flow data

M. Togneri, I. Masters, and A. J. Williams

***Abstract*—ADCPs are the conventional instrument for estimation of mean flow properties at tidal stream sites, but have some difficulties with measurement of turbulence. One particular issue arises with estimating the strength of the turbulent kinetic energy: it is not *a priori* possible to separate velocity fluctuations driven by turbulence from those driven by waves. A previous study has shown a novel method to decouple these effects in real field data, but could only be assessed against the wave component as no independent measure of the turbulent component was possible. In this study, we describe the generation of synthetic flowfields sampled by 'virtual' ADCPs to assess the performance of the novel filter method against the turbulent component. The method is shown to significantly outperform some but not all existing methods.**

***Index Terms*—ADCPs, turbulence, turbulent kinetic energy, measurement error**

I. Introduction

ACCURATE assessment of marine currents is critical for meaningful planning of tidal stream energy deployments. Methods for assessing mean flow speed are well-established [1], but the issue of assessing phenomena that vary over much shorter time scales than the semidiurnal tide (principally turbulence and waves) is not as settled. This is in part due to the limitations of the standard instruments used for surveying currents at potential tidal stream sites i.e., acoustic Doppler current profilers (ADCPs). Because ADCPs use multiple acoustic beams to sample single components of velocity at widely-separated spatial locations, a reliable analysis of the mean flow can be obtained by a suitable average over measurements from all beams: this approach works well for determining mean flow properties, but is less well-suited for the smaller and faster variations associated with waves and turbulence. In particular, conventional analysis approaches such as the variance method do not meaningfully distinguish between wave-driven and turbulence-driven velocity variations.

An important consequence of this is that ADCP estimates of turbulent kinetic energy (TKE, or k) are biased high because the TKE calculation method includes wave-driven velocity fluctuations as well as those caused by turbulence. This is intuitive when we consider the definition of k:

$$k = \tfrac{1}{2}\left(\langle u'^2\rangle + \langle v'^2\rangle + \langle w'^2\rangle\right), \quad (1)$$

where u, v, w are the Cartesian components of velocity and a prime indicates the fluctuating component of a flow quantity after Reynolds decomposition. This definition holds true as long as the fluctuations around the mean are due only to turbulent action. The averaging period for ADCP data, however, is significantly longer than swell periods: therefore the fluctuating component of ADCP velocity measurements at tidal sites with significant wave action will also include wave-driven velocities.

The ADCP estimate of k can thus be thought of a superimposition of the "true" TKE k_t and a wave pseudo-TKE k_w i.e., $k_{ADCP} = k_t + k_w$. Earlier attempts to decouple waves and turbulence have relied on a significant separation of vertical length scales (e.g., the 'adaptive filtering' method described in [2] and [3]) which is not typical of sites suitable for tidal energy extraction, or on fitting an expected turbulent spectrum to along-beam velocity measurements [4]. Although this cospectral fitting has a solid physical basis, it often fails to find an appropriate fit (e.g., less than half the measurements in [5]).

Previous work by the authors [6] has successfully applied a mixed spectral-statistical filter to ADCP estimates of TKE from a tidal stream test site; this filter showed good performance in distinguishing between true TKE and pseudo-TKE due to wave action. In particular, this model showed that it was possible to more accurately reconstruct wave pseudo-TKE using the spectral-statistical filter than with previous single-method filters. However, for field data it is only possible to assess the filter's performance with respect to wave pseudo-TKE: this is because independent measurements of wave properties can be obtained from a surface buoy, but there is no alternative instrumentation that can yield independent measurements of turbulence.

Because the wave pseudo-TKE is strongly dominant in ADCP estimates of TKE at tidal sites with significant wave action, we hypothesised that the improvement in accuracy for the true turbulent TKE may be greater

This work was carried out under the WTIMTS project, funded by EPSRC via the Supergen ORE Hub Flexible Funding scheme, EP/S000747/1, and under the SELKIE project funded by the European Regional Development Fund via the Ireland Wales Cooperation Programme.

Authors are affiliated with the Energy and Environmental Research Group in the Faculty of Science and Engineering at Swansea University Bay Campus, Fabian Way, Swansea SA1 8EN, UK (contact e-mail: M.Togneri@swansea.ac.uk).

Digital Object Identifier:
https://doi.org/10.36688/ewtec-2023-467

than the improvement in accuracy for wave pseudo-TKE. In order to test this hypothesis, we need a suitable flowfield (i.e., one with both significant turbulence and wave action) for which it is possible to obtain a second measurement of turbulence independent of the ADCP. Such measurements are not available in the field, so we have investigated the problem in a different way: we generate a synthetic flowfield with known turbulence and wave properties, and test the filter's performance on measurements from a "virtual ADCP" that samples this velocity data.

II. Methods

A. Synthetic flow generation

The synthetic flowfield is generated following the procedure of Crossley et al [7], [8]. This approach starts by defining the space in which the virtual ADCP is intended to operate, and the points within that space corresponding to the bin centres of each beam of the virtual ADCP. For all of these points, a time series of velocities is generated based on a specified mean flow profile and a specified wave spectrum. In all cases presented here, the mean flow is a simple 1/7th power law profile; two kinds of wave velocity fields are investigated, one monochromatic and one based on the JONSWAP spectrum [9]. At this point, we directly calculate the wave pseudo-TKE profile (i.e., $k_w(z)$, where z denotes vertical position in the water column) of the virtual flowfield without any turbulent action, simply by using the known Cartesian velocity components in equation 1 in a column directly above the location of the virtual ADCP.

We then use a library of pre-generated records of normalised turbulent fluctuations to add turbulence. Each record is generated using the spectral approach conventionally known as the "Sandia method", first reported by Veers [10]. This specifies a two-dimensional grid of points on a plane orthogonal to the mean flow direction. For each point, we specify a turbulent spectrum and a coherence with all other points in the grid; for the cases presented here, this is the standard von Kármán spectrum [11]. Although this was originally developed to describe turbulence in the atmospheric boundary layer, previous studies have shown that it also performs well in describing turbulent flowfields at sites with strong tidal flows [12]. The original paper by Veers also gives a semi-empirical function to define cross-coherence between points; in the absence of more specific information this is employed for the current study.

From the spectra and cross-spectra we define a series of amplitudes for each point on the grid and associate a random phase to each coefficient, yielding a series of Fourier coefficients on which we perform an inverse transform to yield a time-series of normalised fluctuations with the correct spectral properties. These normalised fluctuations can then be superimposed on the combined mean current and wave flowfield by interpolating from the grid to the virtual ADCP sample locations; interpolation along the streamwise direction is made possible by applying Taylor's frozen turbulence hypothesis to establish an equivalence between elapsed time and along-stream displacement. The total synthetic TKE k is calculated from the combined flowfield in the same way as the wave pseudo-TKE, described above; the true TKE k_t of the synthetic flowfield is calculated simply by subtracting k_w from k.

We have made two principal extensions to the procedure as described in [7] and [8]. The first and simpler of these extensions is to allow the output of multiple sample depths simultaneously using the same randomised wave and turbulence properties; this was outwith the scope of the previous study, but is necessary here in order to meaningfully apply the statistical filter (see section II-B). The second extension is to generate a series of synthetic flowfields that resemble the flow conditions sampled by real ADCPs operated on a typical duty cycle.

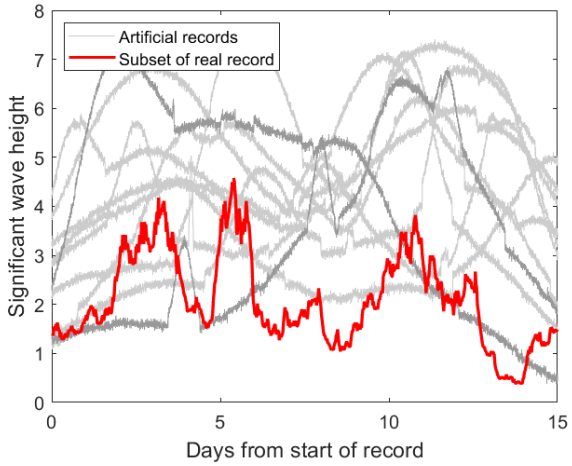

Fig. 1. Comparison of artificial wave height records of 15 days' duration with a subset of a real wave height record used in a previous study [13]. Artificial records corresponding to representative results shown in section III are shown in darker grey.

To define this series of synthetic flowfields, we specify:

- The duration of the deployment - for the current study, this is fifteen days i.e., the minimum number of complete days required to cover a spring-neap cycle
- The duty cycle i.e., how the ADCP alternates between sampling periods and rest periods - for the current study, this was one fifteen-minute sampling burst in every hour of the deployment
- Suitable mean flow properties for each sampling period i.e., mean water depth, mean current speed, significant wave height and mean wave period

The mean water depth and current speed are approximated as a simple superimpositions of an M_2 constituent of period 12.42 hours and a "spring-neap" constituent (approximating the combined long-term effect of other diurnal and semi-diurnal tidal constituents) of period 14.77 days. The amplitude of these two

constituents can be altered to represent different virtual sites. Since we allow only the mean current speed to vary from period to period and not the direction, we are restricted to considering only sites where the flood and ebb are perfectly bidirectional. Some examples of artificial wave height records are compared with a record of the same duration from a real site in figure 1; the real data is taken from a site off the coast of Anglesey in the Irish Sea [13], but we have chosen to simulate conditions more typical of a south-western Welsh site with stronger wave activity.

B. Wave-turbulence separation

As established in the introduction, the purpose of generating a series of synthetic flowfields with associated virtual ADCP measurements is to validate a novel method of decoupling wave and turbulent action in ADCP measurements of TKE. This method, which combines spectral and statistical techniques, builds on an approach which is described in detail by the authors in an earlier paper [13], based solely on empirical orthogonal function (EOF) analysis. The spectral-statistical method, which augments the purely statistical approach by additionally filtering wave action using spectral properties of the ADCP measurements, is outlined in a paper from a previous edition of this conference [6]. The key principle is that wave-turbulence decoupling can be improved by attempting separation both in the frequency and time domains. Frequency-domain separation is applied to relatively short time series of velocity measurements, whereas time-domain separation is applied to the whole ADCP deployment record. We provide only a brief description of the method here; please refer to the earlier publications for a fuller explanation.

The standard way to estimate TKE from ADCP measurements is with the variance method. By assuming that *(a)* first- and higher-order statistical moments of all velocity components are spatially homogeneous across the horizontal spread of the beams, and *(b)* these statistical properties are also approximately stationary for averaging periods sufficiently short in comparison to the dominant tidal constituents, we can restate the definition of k in equation 1 such that it is expressed in terms of along-beam velocity variances:

$$k_{ADCP} = \frac{\sum_{i=1}^{4} \langle b_i'^2 \rangle}{4 \sin^2\theta \left(1 - \xi \left(1 - \cot^2\theta\right)\right)}. \qquad (2)$$

Here, b_i is the measured along-beam velocity for the ith beam, θ is the angle between each of the ADCP's beams and the vertical, and ξ is a variable that parametrises the anisotropy of the turbulence.

The spectral-statistical method first applies a filter to the spectra of each along-beam velocity record. This filter uses a wavelet synchrosqueeze transform (WSST) [14] to search for peaks in spectral energy; if these peaks appear to be associated with wave action, the filter will stop a portion of the energy around this peak and pass the remainder. A well-designed filter will resolve a significant portion of the wave energy into the stopped portion, with the passed portion containing the "true" turbulent action in the frequency domain plus some residual wave action.

The stopped and passed portions of the spectra are then both transformed back into the time domain and equation 2 is applied to estimate the TKE corresponding to each portion. If the filter works as expected, the stopped portion should contain only velocity fluctuations associated with wave action: therefore, the component of TKE obtained from this is denoted $k_{w,1}$ i.e., the first part of the wave pseudo-TKE. We also estimate the TKE associated with the filter-passed portion, which we denote k_{FP}, and then apply the EOF-based method to the whole-record k_{FP} distribution. This decomposition should yield the true turbulent TKE k_t and the remaining part of the wave pseudo-TKE, $k_{w,2}$. Finally, the estimate of total wave pseudo-TKE is simply the sum $k_w = k_{w,1} + k_{w,2}$.

III. Results

As mentioned in section II-A, we investigate flows with two different types of sea state: a simple monochromatic wave ("regular") and a more realistic distribution of wave energy over multiple frequencies using the JONSWAP spectrum ("irregular"). We have generated six virtual records of both regular and irregular types. We first present results giving a representative overview of the behaviour of the various estimates of TKE, before going on to analyse their performance quantitatively.

A. Distributions of k, k_{ADCP}, k_t and k_w

In figures 2 and 4, we show the "true" total synthetic TKE k of calculated directly from the flowfield velocities in representative regular and irregular sea states, alongside their decomposition into turbulent k_t and wave k_w components following the procedure described in II-A. It is clear that with both types of wave conditions, the wave pseudo-TKE is of much greater magnitude than the true turbulence at times of strong wave activity. Note that in the irregular sea state, the decomposition yields some negative k_t values, which appear as blank spaces in these figures because we use of log values for the contours.

The final panels of these figures show the value of total TKE estimated by the virtual ADCPs, k_{ADCP}. Note that these estimates differ from the true total TKE, consistent with the observations of [7], although we do not consider here the individual components of turbulence intensity. Characterising the discrepancy between k_{ADCP} and k is not straightforward, as it depends both on depth and the strength of wave activity.

Figures 3 and 5 show the results of applying the two filtration methods independently and together to estimate the k_t and k_w components. Note that the EOF method requires all profiles to contain the same

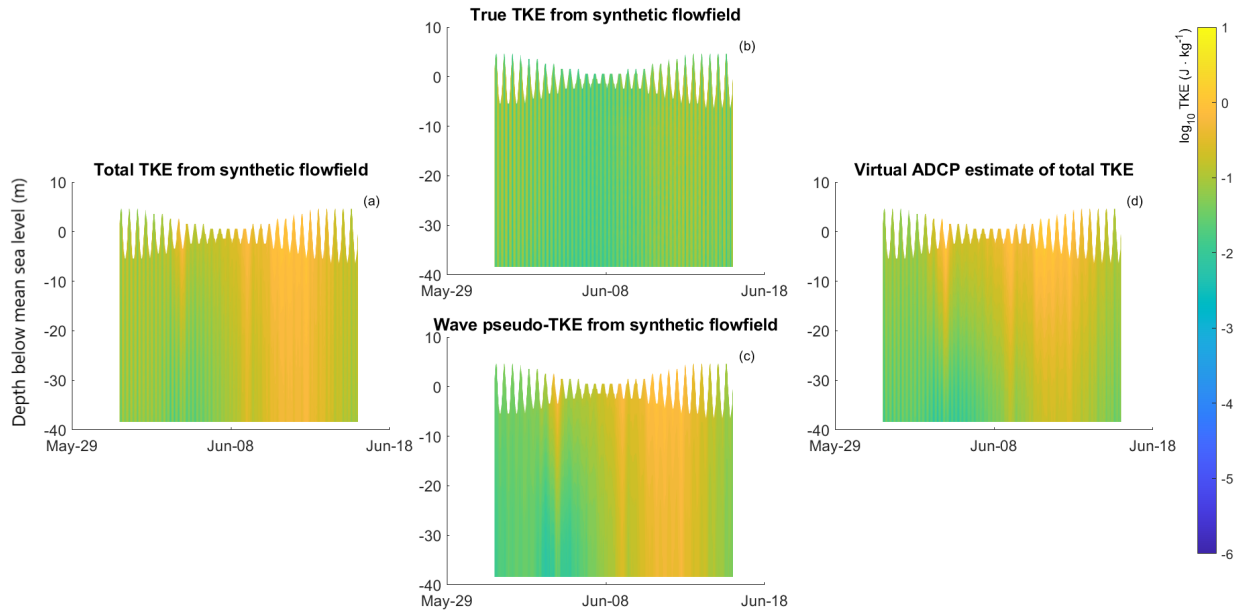

Fig. 2. Contour plots of total TKE values and known components ($\log_{10} k$) calculated directly from the synthetic velocities for a representative regular sea state case. Panel (a): Total TKE (k). Panel (b): True TKE (k_t). Panel (c): Wave pseudo-TKE (k_w). Panel (d): Estimate of total TKE from the virtual ADCP (k_{ADCP})

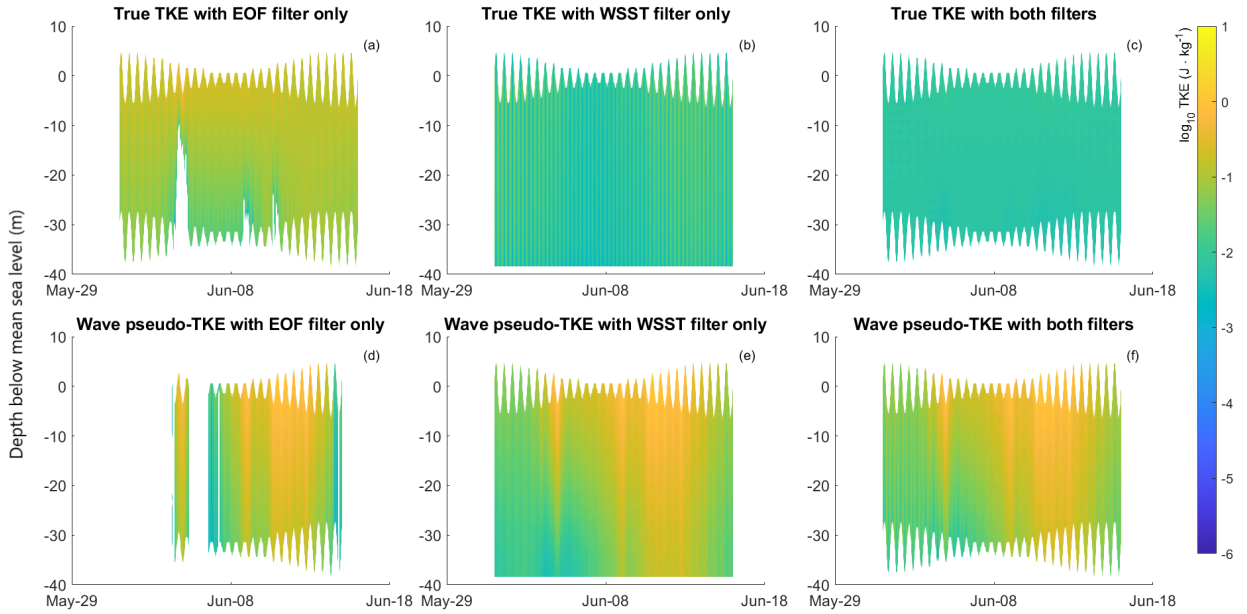

Fig. 3. Contour plots of TKE components ($\log_{10} k$) estimated from virtual ADCP data using different filtering methods for a representative regular sea state case. Panel (a): True TKE (k_t) with EOF/statistical filter only. Panel (b): True TKE (k_t) with WSST/spectral filter only. Panel (c): True TKE (k_t) with both filters. Panel (d): Wave pseudo-TKE (k_w) with EOF/statistical filter only. Panel (e): Wave pseudo-TKE (k_w) with WSST/spectral filter only. Panel (f): Wave pseudo-TKE (k_w) with both filters.

number of data points, which results in some loss of data near the bed in the EOF and double-filtered cases.

In both regular and irregular sea states it is clear that the EOF filter alone performs quite poorly (cf. panels (a) and (d) of both figures), and this is borne out in the analysis of the errors presented later. Both the WSST-only and combined filters reconstruct the gross features of the specified k_w distribution (panels (e) and (f)), but their performance with respect to k_t differs.

In a regular sea state, applying the WSST filter alone yields a k_t estimate with a clear diurnal variation and no evidence of near-surface maxima or transient maxima associated with wave activity - cf. panel (b) of figure 3. However, when using both filters, the k_t estimate is near-uniform - see panel (c) of the same figure. For the irregular sea state, on the other hand, the WSST filter alone does not fully remove the wave activity; it is clear that some of the higher-energy wave events (e.g., around 2-3 days into the synthetic record) are not fully removed from the estimate of k_t shown in panel (b) of figure 5. With both filters applied to the irregular case, however, the distribution of k_t much more closely resembles its

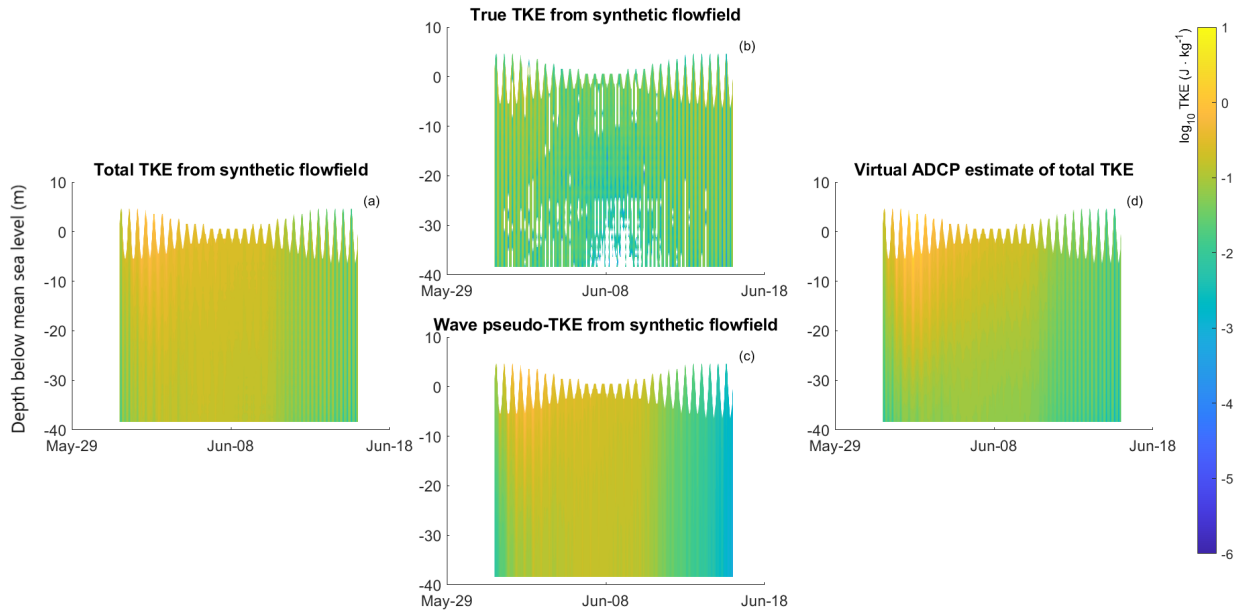

Fig. 4. Contour plots of total TKE values and known components ($\log_{10} k$) calculated directly from the synthetic velocities for a representative irregular sea state case. Panel (a): Total TKE (k). Panel (b): True TKE (k_t). Panel (c): Wave pseudo-TKE (k_w). Panel (d): Estimate of total TKE from the virtual ADCP (k_{ADCP})

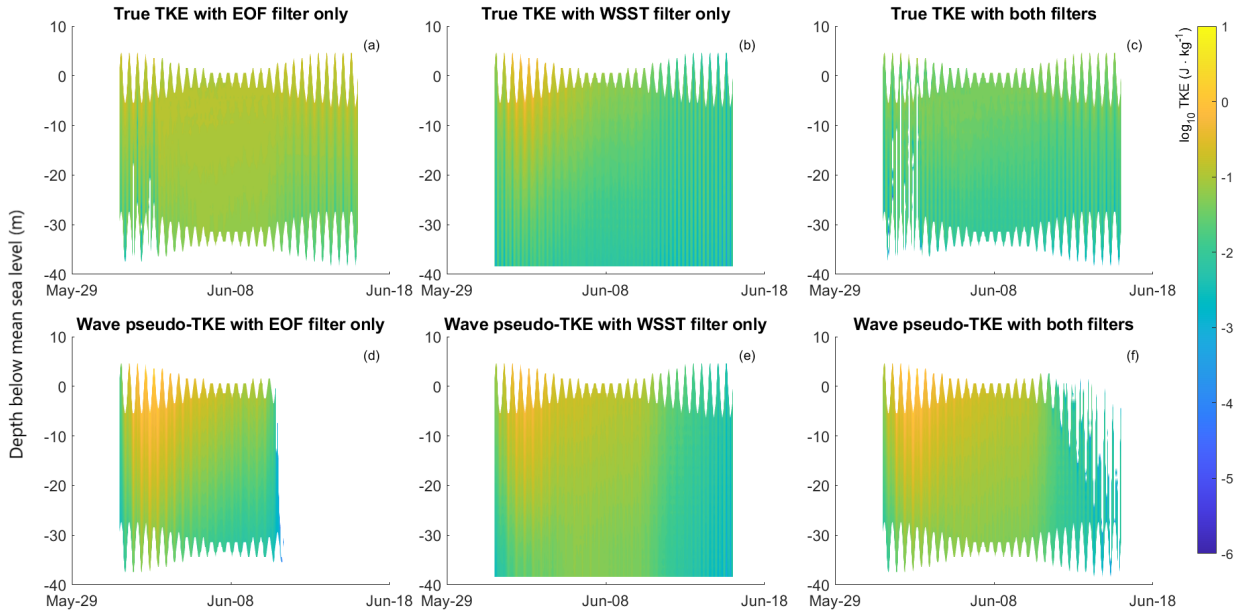

Fig. 5. Contour plots of TKE components ($\log_{10} k$) estimated from virtual ADCP data using different filtering methods for a representative irregular sea state case. Panel (a): True TKE (k_t) with EOF/statistical filter only. Panel (b): True TKE (k_t) with WSST/spectral filter only. Panel (c): True TKE (k_t) with both filters. Panel (d): Wave pseudo-TKE (k_w) with EOF/statistical filter only. Panel (e): Wave pseudo-TKE (k_w) with WSST/spectral filter only. Panel (f): Wave pseudo-TKE (k_w) with both filters.

expected value (i.e., the distribution shown in panel (b) of figure 4).

B. Error estimation

To assess how well each filter performs, we calculate the error of each estimate of k_t and k_w with respect to its expected value i.e., the distributions of k_t and k_w calculated directly from the known velocities of the synthetic flowfields, as described in section II-A. We calculate the average error for each profile (i.e., the profiles calculated for each synthetic flowfield of fifteen minutes' duration), and then further average the profile error over the whole record to get a single estimate of error for each record. Finally, we average again over all six realisations of the irregular and regular sea states to obtain the 'overall' error estimates that are presented in figures 6 and 7.

We see in figure 6 that the EOF estimates of both k_t and k_w have much higher errors than either the WSST estimates or the estimates obtained with both filters; this is consistent with its apparent poor performance in the representative cases visualised in figures 3 and 5. The absolute error in k_w is slightly improved by using the combined filter rather than the WSST filter

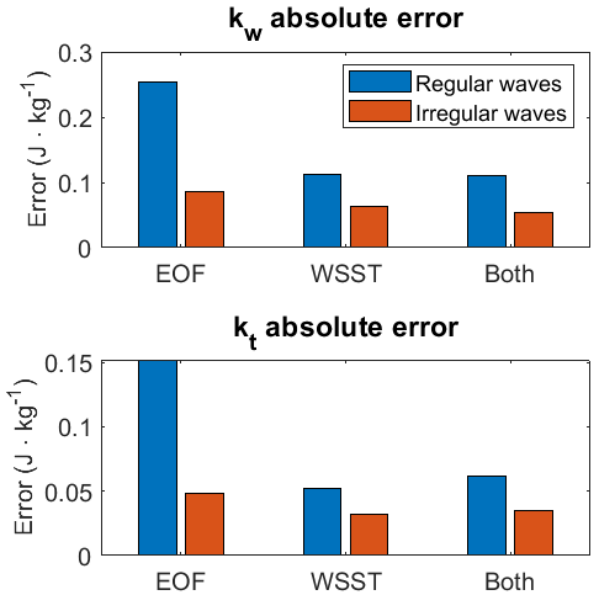

Fig. 6. Absolute error for (top) k_w and (bottom) k_t in both regular and irregular waves with different filters applied

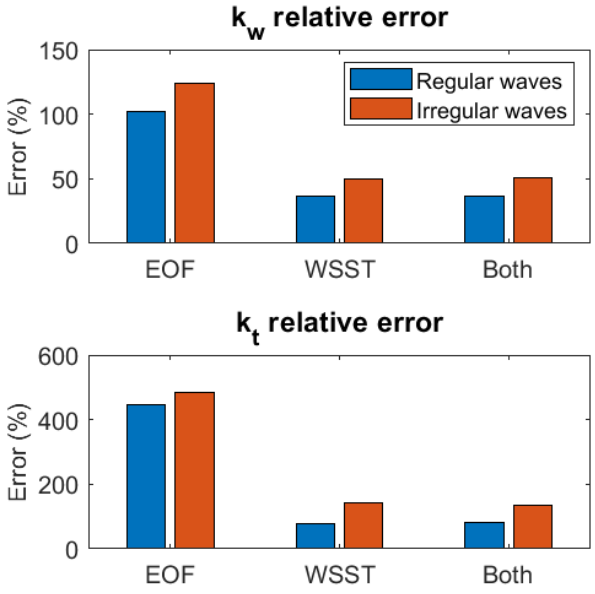

Fig. 7. Relative error for (top) k_w and (bottom) k_t in both regular and irregular waves with different filters applied

alone for both regular and irregular waves (top panel of figure 6), but this is reversed for k_t. For all filtering approaches, absolute error is much smaller when attempting wave-turbulence separation in an irregular sea state.

The relative error, however, shows the opposite behaviour: relative error is smaller in regular waves than in irregular waves for all filters. To examine possible explanations for this, figures 8 and 9 show relationships between the relative error and the absolute error, and also between the relative error and the underlying k_t or k_w values (i.e., those calculated directly from the synthetic flowfield) that the error corresponds to. These scatter plots are drawn from only a single instance of a regular or irregular sea state, the same instances that are used for the representative visualisations shown in figures 2 to 5.

In all cases there appears to be little obvious difference for the behaviour of the EOF error between regular and irregular cases, which is consistent with the relatively small differences seen for the EOF relative errors in the leftmost bars in both panels of figure 7. For both the WSST and combined-filter errors, there is a clear change in the relationship between relative and absolute errors in k_t when moving from a regular sea state to an irregular one; this can be seen by comparing the top-left panels of figure 8 with the corresponding panels in figure 9. In regular wave conditions, there is a sharp reduction in relative error as absolute error gets smaller; this is particularly evident for the combined-filter case. This is not present for the irregular sea state; although there is a small reduction in relative error for the very smallest values of absolute error, there is a strong peak in relative error for absolute errors between 0.1 and 0.25 $J \cdot kg^{-1}$.

The relationship between relative error and k_t is similar, although the peak of relative error coincides with the very smallest values of k_t rather than the near-smallest values. Relative error in k_w, on the other hand, does not show any qualitative difference between regular and irregular wave conditions. In both types of sea state, it is clear that the relative error becomes larger for low values of both absolute error and underlying k_w; the difference appears to be simply one of magnitude, with the relative error peaking at much greater magnitudes but corresponding to roughly the same values of absolute error and k_w.

IV. Discussion and Conclusions

The virtual ADCP sampling procedure described in section II-A yields a time series of all three components of velocity for points at the centre of every ADCP sampling cell. This is a simplification of the true situation for a number of reasons: a real ADCP's measurement of the velocity in a single cell is an average of the velocity from all scatterers within the ensonified volume of the cell; neighbouring cells have overlapping volumes and so their correlation is augmented beyond what would be expected from the underlying physics alone; and random Doppler noise arising from scatterers moving in and out of the ensonified volume during measurement is not accounted for. It is difficult to anticipate exactly how accounting for these effects might alter the results found here, but this would be a valuable extension to this work.

The unusual behaviour of the WSST filter's estimates of k_t for regular sea states, and its consequences for the combined filter's results, is described at the end of section III-A. Although the qualitative difference is

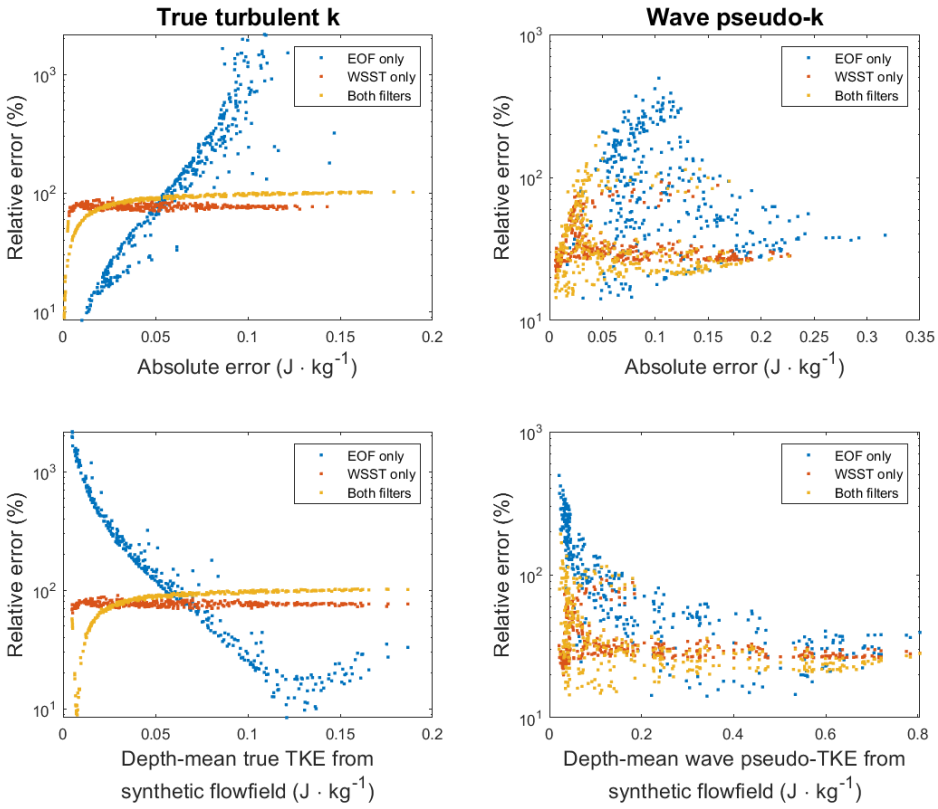

Fig. 8. Scatter plots showing the relationship of relative error with absolute error and underlying k component for different filters in a representative regular wave case. Left-hand panels show k_t, and right-hand panels show k_w; top panels show relationship with absolute error, and bottom panels show relationship with the underlying k_t or k_w values calculated directly from the synthetic velocity field

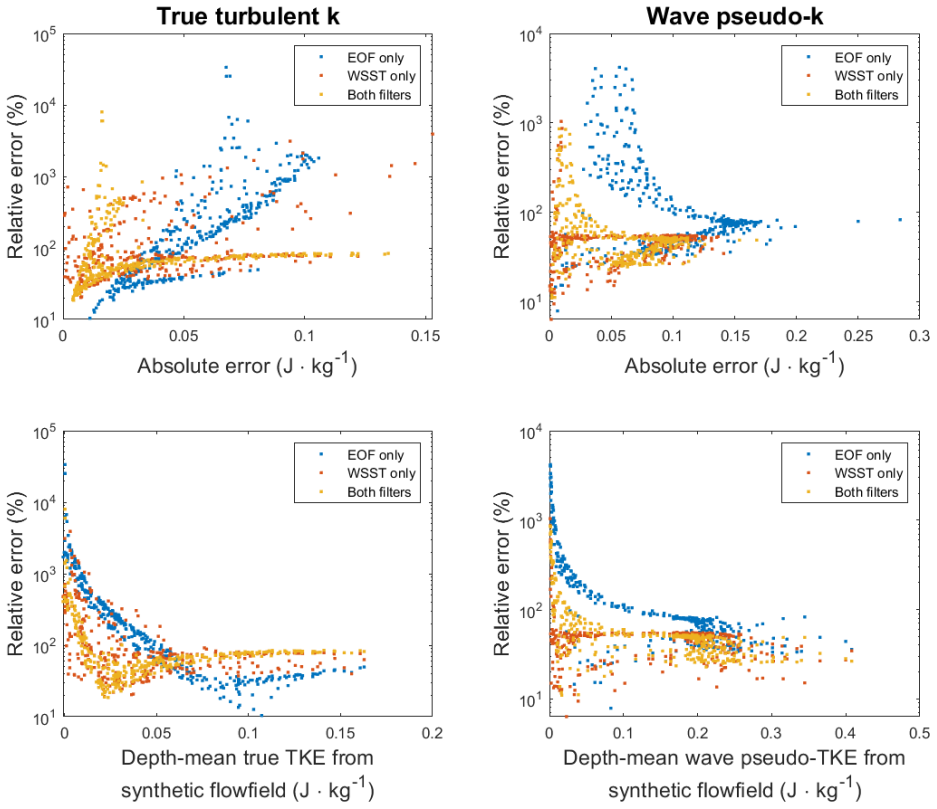

Fig. 9. Scatter plots showing the relationship of relative error with absolute error and underlying k component for different filters in a representative irregular wave case. Left-hand panels show k_t, and right-hand panels show k_w; top panels show relationship with absolute error, and bottom panels show relationship with the underlying k_t or k_w values calculated directly from the synthetic velocity field

not borne out in the absolute errors shown in figure 6 in particular, the difference in the k_t estimates in panels (b) and (c) of figures 3 and 5 is striking. It appears that for regular sea states (i.e., where there is a single wave frequency) it is much easier for the WSST filter to identify and separate the spectral peak associated with the wave activity; this is perhaps intuitive. As a result, the WSST filter's estimate of k_t does not contain any clearly wave-like features. The EOF filter (which is applied after the WSST filter in the combined case, cf. section II-B) relies on the presence of a data mode that approximates a physical mode. A distribution of filter-passed TKE k_{FP} that does not retain any wave-like features, therefore, will not have any suitable data modes to isolate and the EOF will not function as intended. This is a potential explanation for why panel (c) of figure 3 appears to show a near-uniform distribution of k_t without any clear features (e.g., semidiurnal variation, near-surface or near-bed maxima, transient maxima associated with high-energy wave events). However, this does not explain why the WSST-only estimate of k_t in fact has a slightly *lower* error compared to the expected value than the combined-filter estimate (cf. the second two blue bars in the bottom panel of figure 6).

It is also interesting that not just the EOF filter, but all filtering methods, perform better with respect to absolute error for irregular sea states, but worse with respect to relative error. In the case of k_t, it appears this is due to the filter performing well for large values of k_t but poorly for near-zero values; this is perhaps acceptable, as it is usually more intense turbulent conditions that are of greater concern for tidal energy sites. For k_w, it is more difficult to discern a reason for the greater relative errors.

The use of synthetic flowfields to test the novel spectral-statistical method for wave-turbulence separation has afforded us insights into its behaviour with respect to known k_t distributions that would not have been possible with field data. This study does not show an advantage for the spectral-statistical method in estimating k_t over a WSST filter alone. Some questions remain open, however: with data from a real field deployment of an ADCP, the combined filter did outperform the EOF filter, but only with careful tuning of the spectral filter properties [6]. It is not then clear why the combined filter shows such a clear improvement over the EOF filter alone with synthetic data, or why the WSST filter alone performs so well. There is clear scope to further refine the generation of synthetic flowfields to better reflect realistic flow conditions, and to investigate the importance of the other real ADCP effects mentioned at the start of this section.

Acknowledgement

In addition to the funder (see title page footnote), the authors would like to thank the steering group of the WTIMTS project for their invaluable feedback on this research. The authors also acknowledge the support of the SEACAMS and SEACAMS 2 projects, part-funded by the European Regional Development Fund through the Welsh Government; the real site data used as a reference for this study were collected by researchers at Bangor University under these research programmes and are hosted on the IMARDIS data portal (www.imardis.org).

References

[1] "Tidal Energy Resource Assessment and Characterisation (IEC 62600-201)," International Electrotechnical Commission, Standard, 2014.

[2] W. J. Shaw and J. H. Trowbridge, "The direct estimation of near-bottom turbulent fluxes in the presence of energetic wave motions," *Journal of Atmospheric and Oceanic Technology*, vol. 18, no. 9, pp. 1540–1557, 2001.

[3] J. H. Rosman, J. L. Hench, J. R. Koseff, and S. G. Monismith, "Extracting Reynolds stresses from acoustic Doppler current profiler measurements in wave-dominated environments," *Journal of Atmospheric and Oceanic Technology*, vol. 25, no. 2, pp. 286–306, 2008.

[4] A. R. Kirincich, S. J. Lentz, and G. P. Gerbi, "Calculating Reynolds stresses from ADCP measurements in the presence of surface gravity waves using the cospectra-fit method," *Journal of Atmospheric and Oceanic Technology*, vol. 27, no. 5, pp. 889–907, 2010.

[5] A. R. Kirincich and J. H. Rosman, "A comparison of methods for estimating Reynolds stress from ADCP measurements in wavy environments," *Journal of Atmospheric and Oceanic Technology*, vol. 28, no. 11, pp. 1539–1553, 2011.

[6] M. Togneri, I. Masters, A. Williams, and I. Fairley, "A spectral-statistical filter for decoupling wave and turbulence effects at tidal sites," in *Proceedings of the European Wave and Tidal Energy Conference*, 2021, pp. 1–1927.

[7] G. Crossley, A. Alexandre, S. Parkinson, A. H. Day, H. C. Smith, and D. M. Ingram, "Quantifying uncertainty in acoustic measurements of tidal flows using a 'virtual'doppler current profiler," *Ocean Engineering*, vol. 137, pp. 404–416, 2017.

[8] G. Crossley, "Quantification of uncertainty in sub-sea acoustic measurement, and validation of wave-current kinematics, at a tidal energy site," Ph.D. dissertation, 2018.

[9] K. Hasselmann, T. P. Barnett, E. Bouws, H. Carlson, D. E. Cartwright, K. Enke, J. Ewing, A. Gienapp, D. Hasselmann, P. Kruseman *et al.*, "Measurements of wind-wave growth and swell decay during the joint north sea wave project (jonswap)." *Ergaenzungsheft zur Deutschen Hydrographischen Zeitschrift, Reihe A*, 1973.

[10] P. S. Veers, "Three-dimensional wind simulation," Sandia National Labs., Albuquerque, NM (USA), Tech. Rep., 1988.

[11] T. Von Karman, "Progress in the statistical theory of turbulence," *Proceedings of the National Academy of Sciences*, vol. 34, no. 11, pp. 530–539, 1948.

[12] I. A. Milne, R. N. Sharma, R. G. Flay, and S. Bickerton, "Characteristics of the turbulence in the flow at a tidal stream power site," *Philosophical Transactions of the Royal Society of London A: Mathematical, Physical and Engineering Sciences*, vol. 371, no. 1985, p. 20120196, 2013.

[13] M. Togneri, I. Masters, and I. Fairley, "Wave-turbulence separation at a tidal energy site with empirical orthogonal function analysis," *Ocean Engineering*, vol. 273, p. 109523, 2021.

[14] G. Thakur, E. Brevdo, N. S. Fučkar, and H.-T. Wu, "The synchrosqueezing algorithm for time-varying spectral analysis: Robustness properties and new paleoclimate applications," *Signal Processing*, vol. 93, no. 5, pp. 1079–1094, 2013.